

# COUPLED THERMOELASTIC ANALYSIS OF BEAM STRUCTURES USING A REFINED 1D FINITE ELEMENT MODEL

M. Filippi<sup>1</sup>, R. Azzara<sup>1</sup>, M. Santori<sup>1</sup>, M. Petrolo<sup>1</sup> & E. Carrera<sup>1</sup>

<sup>1</sup>Mul2 Lab, Department of Mechanical and Aerospace Engineering, Politecnico di Torino , Corso Duca degli Abruzzi 24, 10129 Torino, Italy.

#### **Abstract**

In this paper, static and dynamic problems in the framework of coupled and uncoupled thermoelasticity are analyzed. A refined one-dimensional (1D) model, based on the Carrera Unified Formulation (CUF), is employed to provide accurate predictions for the displacement and temperature change fields within homogeneous isotropic structures under thermal loadings. This approach offers the distinct advantage of transforming the complex three-dimensional (3D) problem into a computationally efficient 1D model, ensuring a balance between precision and reduced computational costs. This work introduces generalized theories of thermoelasticity, specifically based on the Lord-Shulman and Green-Lindsay models. Other cases such as static, quasi-static and dynamic can be seen as particular cases of this generalized formulation. The study focuses on a simplified configuration, employing variable kinematics models, such Lagrange polynomial and Taylor expansion functions. Numerical solutions and convergence studies are presented to demonstrate the accuracy of the formulation.

**Keywords:** Carrera Unified Formulation; coupled thermoelasticity; finite element method.

## 1. Introduction

In aeronautics, a large number of problems require the study of thermal stresses. Components are often subjected to very high temperatures or large temperature variations. Such problems can be solved according to different models.

In static uncoupled thermoelasticity, the stationary temperature distribution determines an effect on deformations. Quasi-static uncoupled thermoelasticity considers the time-dependent temperature distributions resulting from the transient thermal conduction equation, which leads to transient thermal stresses. In contrast, dynamic uncoupled thermoelasticity incorporates inertia effects when external thermomechanical loads vary rapidly over time. In uncoupled theories, temperature is obtained independently directly from the heat conduction equation, while displacements are partly due to the effect of temperature.

However, the uncoupled approach does not always make it possible to realistically evaluate the behaviour of a structure when, for example, it is subjected to rapid and high thermomechanical loads. In fact, in this case, the effects of deformations on temperature and inertial forces are no longer negligible. Hence, the need to use more sophisticated theories of coupled thermoelasticity.

Introduced by Duhamel [1] in 1837, the coupling effect in the equations of thermoelasticity was later studied by Biot, who in 1956 presented the theory of classical thermoelasticity [2]. According to the classical theory, thermal disturbances propagate with infinite speed through the body. Because of this nonphysical behaviour, several coupled thermoelasticity models have been developed that overcome the limitations of the classical model. The Lord-Shulman (LS) and Green-Lindsay (GL) models are among these [3–5].

The analytical solution of these coupled equations is usually available only for simple configurations and boundary conditions [6–8], which has led to an increasing reliance on numerical methods such

as the FEM. The FE formulation of the thermoelastic governing equations can be obtained through the Principle of Virtual Displacements (PVD) [9].

For complex configurations, 1D and 2D models do not always provide the accuracy the problem requires. The three-dimensional nature of the problem demands solid models, incurring high computational costs. A refined one-dimensional model in the framework of Carrera Unified Formulation [9–14] is used in this work. This approach was implemented first for the plate and shell [15] and later for the beam [16]. CUF allowed, compared to the 1D and 2D FE models usually used, to achieve accuracy comparable to solid models while maintaining a low computational cost. In addition, another strength of CUF is the ability to analyze multi-field problems (mechanical, thermal, electrical) [17–19] with high accuracy. Recently, CUF has also been used for thermoelastic analysis on beams and disks [20–22]. This paper aims to show the use of 1D FE-CUF models in the context of three-dimensional coupled thermoelasticity problems. In particular, some numerical results related to static and quasi-static problems are proposed.

# 2. Equations and models

# 2.1 Governing equations

The equation of motion in a three-dimensional domain is expressed as in [23,24]:

$$\sigma_{ij,j} + X_i = \rho \ddot{u}_i + \zeta \dot{u}_i \tag{1}$$

where  $\sigma_{ij}$  is the stress component,  $u_i$  is the displacement component and  $X_i$  denote the volume forces.  $\rho$  and  $\zeta$  are the density and damping coefficient, respectively. In the chosen notation, the derivative in time is denoted by the superscript  $(\cdot)$  while the derivative in space by the subscript  $(\cdot)$ . According to Hooke's law for a nonhomogeneous anisotropic material, the stress component is expressed as:

$$\sigma_{ij} = C_{ijpq} \varepsilon_{pq} - \beta_{ij} (T + t_1 \dot{T}) \tag{2}$$

where  $C_{ijpq}$  is the 4-order elasticity tensor, T is the temperature change with respect to the reference temperature  $T_0$  and  $t_1$  is one of the two relaxation times predicted by Green-Lindsay (GL) theory . Strains  $\varepsilon_{ij}$  can be expressed as a function of displacements:

$$\varepsilon_{ij} = \frac{1}{2}(u_{i,j} + u_{j,i}) \tag{3}$$

The thermo-stress module  $\beta_{ij}$  can be written as:

$$\beta_{ij} = C_{ijpq} \alpha_{pq} \tag{4}$$

where  $\alpha_{pq}$  is the thermal expansion coefficient.

The energy equation can be expressed through the following relationship:

$$q_{i,i} = R - T_0 \dot{S} \tag{5}$$

where  $q_i$  is the component of heat flux, R denotes the internal heat per unit volume and time and S is the entropy per unit volume. S can be expressed as:

$$S = \frac{\rho c}{T_0} (T + t_2 \dot{T}) + \beta_{ij} \varepsilon_{ij} - \frac{1}{T_0} \tilde{c}_i T_{,i}$$
(6)

The energy equation can be rearranged and written as a function of displacements and temperature [24]:

$$\rho c(t_0 + t_2)\ddot{T} + \rho c\dot{T} - 2\tilde{c}_i\dot{T}_{,i} - (\kappa_{ij}T_{,j})_{,i} + t_0T_0\beta_{ij}\ddot{u}_{i,j} + T_0\beta_{ij}\dot{u}_{i,j} = R + t_0\dot{R}$$
(7)

Parameter c is the specific heat,  $t_0$  and  $t_2$  are the relaxation times relative to LS theory and GL theory, respectively, and  $\tilde{c}$  is a vector of new constants of the material. The thermal conductivity tensor is indicated by the parameter  $k_{ij}$ .

The equations written above are in the most general form possible. In the LS theory case only the relaxation time  $t_0$  is nonzero ( $t_1 = t_2 = \tilde{c}_i = 0$ ), while in the GL case only  $t_0 = 0$ . Since they are coupled, the governing equations must be solved simultaneously.

# 2.2 Principle of Virtual Displacements

To derive the finite element formulation, the principle of virtual displacements (PVD) is used. For the coupled thermoelastic case, the PVD has the following form [9]:

$$\int_{V} (\delta \boldsymbol{\varepsilon}_{p} \boldsymbol{\sigma}_{p} + \delta \boldsymbol{\varepsilon}_{n} \boldsymbol{\sigma}_{n} + \delta T S) dV = \delta L_{ext} - \delta L_{ine}$$
(8)

By convention, subscript p is used for in-plane components, while subscript n denotes out-of-plane components. The vectors  $\boldsymbol{\varepsilon}$  and  $\boldsymbol{\sigma}$  represent the components of strain and stress. S is the entropy per unit volume.  $\delta L_{ext}$  and  $\delta L_{ine}$  are the external and inertial virtual works, respectively.

# 2.3 CUF form of governing equations

The 1D FE model involves discretizing the structure along the *y*-axis of the beam into a number of finite elements. According to the FEM, the displacement and temperature change fields can be written as:

$$\mathbf{u} = N_m \mathbf{u}^m$$

$$T = N_m T^m$$
(9)

where  $N_m$  are the shape functions,  $\mathbf{u}^m$  and  $T^m$  are the vector of displacements and temperature change in the m-th node in the element. Depending on the number of nodes in the beam element, one can have a linear (2-nodes), quadratic (3-nodes) and cubic (4-nodes) interpolation function of temperature and displacements along y-axis.

The displacements and temperature change in the individual node of the beam can be expressed by the distribution of the displacements and temperature over the cross section:

$$\mathbf{u}^{m} = F_{\tau} \mathbf{U}^{m\tau}$$

$$T^{m} = F_{\tau} \mathbf{\Theta}^{m\tau}$$
(10)

where  $F_{\tau}$  are the generic expansion functions,  $\mathbf{U}^{m\tau}$  is the generalized vector of displacements, and  $\Theta^{m\tau}$  is the generalized temperature change. The parameter  $\tau$  denotes the number of terms of the expansion. Taylor expansion (TE) and Lagrange expansion (LE) functions can be used. Lagrange expansions involve discretizing the section using different types of elements for example a biquadratic nine-node (1L9) or bicubic 16-node (1L16) elements. According to the Taylor expansions, the number of terms depends on the order of the model.

Using the geometric and Hooke's equations (Eqs. 2 and 3) and substituting Eqs. 9 and 10 within the Principle of Virtual Displacements (8), the following system written in matrix form is obtained [24]:

$$\begin{bmatrix}
\mathbf{M}_{UU}^{lm\tau s} & 0 \\
\mathbf{M}_{\theta U}^{lm\tau s} & \mathbf{M}_{\theta \theta}^{lm\tau s}
\end{bmatrix} \begin{pmatrix} \ddot{\mathbf{U}}^{ls} \\ \ddot{\Theta}^{ls} \end{pmatrix} + \begin{bmatrix}
\mathbf{G}_{UU}^{lm\tau s} & \mathbf{G}_{U\theta}^{lm\tau s} \\
\mathbf{G}_{\theta U}^{lm\tau s} & \mathbf{G}_{\theta \theta}^{lm\tau s}
\end{bmatrix} \begin{pmatrix} \dot{\mathbf{U}}^{ls} \\ \dot{\Theta}^{ls} \end{pmatrix} + \begin{bmatrix}
\mathbf{K}_{UU}^{lm\tau s} & \mathbf{K}_{U\theta}^{lm\tau s} \\
0 & \mathbf{G}_{\theta \theta}^{lm\tau s}
\end{bmatrix} \begin{pmatrix} \mathbf{U}^{ls} \\ \Theta^{ls} \end{pmatrix} = \begin{Bmatrix} \mathbf{F}^{ls} \\ Q^{ls} \end{Bmatrix}$$
(11)

where the terms of the matrices are expressed through fundamental nucleus, a condensed notation that does not depend on model order or expansion type:

$$[\mathbf{M}_{UU}^{lm\tau s}]_{3x3} = \int_{L^{e}} \int_{A^{e}} (\rho N_{m} N_{l} \mathbf{I} F_{\tau} F_{s}) dA dL$$

$$[\mathbf{M}_{\Theta U}^{lm\tau s}]_{1x3} = \int_{L^{e}} \int_{A^{e}} (t_{0} T_{0} N_{m} N_{l} [\boldsymbol{\beta}_{p}^{T} (\mathbf{D}_{p} F_{s}) + \boldsymbol{\beta}_{n}^{T} (\mathbf{D}_{np} F_{s})] F_{\tau}) dA dL$$

$$+ \int_{L^{e}} \int_{A^{e}} (t_{0} T_{0} [\boldsymbol{\beta}_{n}^{T} N_{m} (\mathbf{D}_{ny} N_{l}) F_{s} F_{\tau}]) dA dL$$

$$[\mathbf{M}_{\Theta U}^{lm\tau s}]_{1x1} = \int_{L^{e}} \int_{A^{e}} (\rho c t_{0} N_{m} N_{l} F_{\tau} F_{s}) dA dL$$

$$+ \int_{L^{e}} \int_{A^{e}} (\rho c t_{2} N_{m} N_{l} F_{\tau} F_{s}) dA dL$$

$$(12)$$

$$[\mathbf{G}_{U}^{lm\tau_{S}}]_{3x3} = \int_{L^{r}} \int_{A^{r}} (\zeta N_{m} N_{l} \mathbf{I} \mathbf{F}_{r} \mathbf{F}_{s}) dA dL$$

$$[\mathbf{G}_{U}^{lm\tau_{S}}]_{3x1} = -\int_{L^{r}} \int_{A^{r}} (t_{1} N_{m} N_{l} [\mathbf{D}_{p}^{T} \mathbf{F}_{r} \mathbf{I}) \boldsymbol{\beta}_{p} + (\mathbf{D}_{np}^{T} \mathbf{F}_{r} \mathbf{I}) \boldsymbol{\beta}_{n} | \mathbf{F}_{s}) dA dL$$

$$-\int_{L^{r}} \int_{A^{r}} (t_{1} (\mathbf{D}_{m}^{T} N_{m}) N_{l} | \mathbf{F}_{r} \boldsymbol{\beta}_{n} \mathbf{F}_{s}]) dA dL$$

$$[\mathbf{G}_{\Theta U}^{lm\tau_{S}}]_{1x3} = \int_{L^{r}} \int_{A^{r}} (T_{0} N_{m} N_{l} | \boldsymbol{\beta}_{p}^{T} (\mathbf{D}_{p} \mathbf{F}_{s}) + \boldsymbol{\beta}_{n}^{T} (\mathbf{D}_{np} \mathbf{F}_{s}) | \mathbf{F}_{r}) dA dL$$

$$+\int_{L^{r}} \int_{A^{r}} (T_{0} [\boldsymbol{\beta}_{n}^{T} N_{m} (\mathbf{D}_{ny} N_{l}) \mathbf{F}_{s} \mathbf{F}_{r}]) dA dL$$

$$[\mathbf{G}_{\Theta \Theta}^{lm\tau_{S}}]_{1x1} = \int_{L^{r}} \int_{A^{r}} (p c N_{m} N_{l} \mathbf{F}_{r} \mathbf{F}_{s}) dA dL$$

$$-\int_{L^{r}} \int_{A^{r}} (2 \tilde{\mathbf{c}}^{T} N_{m} [\mathbf{V}_{n} N_{l}] \mathbf{F}_{r} \mathbf{F}_{s}) dA dL$$

$$-\int_{L^{r}} \int_{A^{r}} (2 \tilde{\mathbf{c}}^{T} N_{m} [\mathbf{V}_{n} N_{l}] \mathbf{F}_{r} \mathbf{F}_{s}) dA dL$$

$$[\mathbf{K}_{UU}^{lm\tau_{S}}]_{3x3} = \int_{L^{r}} \int_{A^{r}} (N_{m} N_{l} [(\mathbf{D}_{np}^{T} \mathbf{F}_{r} \mathbf{I}) [\mathbf{C}_{m} (\mathbf{D}_{np} \mathbf{F}_{s} \mathbf{I}) + \mathbf{C}_{np} (\mathbf{D}_{p} \mathbf{F}_{s} \mathbf{I})]$$

$$+ (\mathbf{D}_{p}^{T} \mathbf{F}_{r} \mathbf{I}) [\mathbf{C}_{pp} (\mathbf{D}_{p} \mathbf{F}_{s} \mathbf{I}) + \mathbf{C}_{np} (\mathbf{D}_{np} \mathbf{F}_{s} \mathbf{I})] dA dL$$

$$+ \int_{L^{r}} \int_{A^{r}} (N_{m} (\mathbf{D}_{ny} N_{l}) [(\mathbf{D}_{np}^{T} \mathbf{F}_{r} \mathbf{I}) \mathbf{C}_{mn} + (\mathbf{D}_{p}^{T} \mathbf{F}_{r} \mathbf{I}) \mathbf{C}_{pn} ]\mathbf{F}_{s}) dA dL$$

$$+ \int_{L^{r}} \int_{A^{r}} ((\mathbf{D}_{n}^{T} N_{m}) N_{l} \mathbf{F}_{r} (\mathbf{D}_{p} \mathbf{F}_{s} \mathbf{I}) + \mathbf{C}_{np} (\mathbf{D}_{np} \mathbf{F}_{s} \mathbf{I})] dA dL$$

$$+ \int_{L^{r}} \int_{A^{r}} ((\mathbf{D}_{n}^{T} N_{m}) N_{l} [\mathbf{F}_{r} \mathbf{F}_{n} \mathbf{F}_{s}]) dA dL$$

$$+ \int_{L^{r}} \int_{A^{r}} ((\mathbf{D}_{n}^{T} N_{m}) N_{l} [\mathbf{F}_{r} \mathbf{F}_{n} \mathbf{F}_{s}]) dA dL$$

$$+ \int_{L^{r}} \int_{A^{r}} (N_{m} N_{l} (\nabla_{p}^{T} \mathbf{F}_{r}) \mathbf{K} (\nabla_{p} \mathbf{F}_{r}) \mathbf{F}_{s}) dA dL$$

$$+ \int_{L^{r}} \int_{A^{r}} (N_{m} N_{l} (\nabla_{p}^{T} \mathbf{F}_{s}) \mathbf{K} (\nabla_{p} \mathbf{F}_{r}) \mathbf{F}_{s}) dA dL$$

$$+ \int_{L^{r}} \int_{A^{r}} (N_{l} (N_{m} N_{l} (\nabla_{p}^{T} \mathbf{F}_{s}) \mathbf{K} (\nabla_{p} \mathbf{F}_{r}) \mathbf{F}_{s}) dA dL$$

$$+ \int_{L^{r}} \int_{A^{r}} (N_{l} (N_{l} N_{l}) (N_{l} \mathbf{K} (\nabla_{p}^{T} \mathbf{F}_{r}) \mathbf{F}_{s}) dA dL$$

$$+ \int_{L^{r}} \int_{A^{r}} (N_{l} (N_{l}$$

in which the matrices  $\mathbf{D}_p$ ,  $\mathbf{D}_{np}$  and  $\mathbf{D}_{nv}$  are:

$$\mathbf{D}_{p} = \begin{bmatrix} 0 & 0 & \partial_{z} \\ \partial_{x} & 0 & 0 \\ \partial_{z} & 0 & \partial_{x} \end{bmatrix}, \quad \mathbf{D}_{np} = \begin{bmatrix} 0 & 0 & 0 \\ 0 & \partial_{z} & 0 \\ 0 & \partial_{x} & 0 \end{bmatrix}, \quad \mathbf{D}_{ny} = \begin{bmatrix} 0 & \partial_{y} & 0 \\ 0 & 0 & \partial_{y} \\ \partial_{y} & 0 & 0 \end{bmatrix}, \tag{16}$$

and the vectors  $\nabla_p$  and  $\nabla_n$  are:

$$\nabla_p = \left\{ \partial_x \quad 0 \quad \partial_z \right\}^T, \quad \nabla_n = \left\{ 0 \quad \partial_y \quad 0 \right\}^T, \tag{17}$$

#### 2.4 Newmark method

The system 11 can be rewritten in compact form as:

$$\mathbf{M}\ddot{\mathbf{q}} + \mathbf{D}\dot{\mathbf{q}} + \mathbf{K}\mathbf{q} = \mathbf{R} \tag{18}$$

where  $\mathbf{q}$  is the vector containing the unknowns of displacements and temperature,  $\mathbf{M}$ ,  $\mathbf{D}$  and  $\mathbf{K}$  are the mass, damping and stiffness matrices, respectively, and finally  $\mathbf{R}$  is the generalized force vector. To solve this system, Newmark's method of integration is adopted [25]. Eq. 19 at time step  $t + \Delta t$  is:

$$\mathbf{M}\ddot{\mathbf{q}}_{t+\Delta t} + \mathbf{D}\dot{\mathbf{q}}_{t+\Delta t} + \mathbf{K}\mathbf{q}_{t+\Delta t} = \mathbf{R}_{t+\Delta t}$$
(19)

The solution of the equation is obtained by assuming that:

$$\dot{q}_{t+\Delta t} = \dot{q}_t + \left[ (1 - \delta) \ddot{q}_t + \delta \ddot{q}_{t+\Delta t} \right] \Delta t$$

$$q_{t+\Delta t} = q_t + \dot{q}_t \Delta t + \left[ \left( \frac{1}{2} - \alpha \right) \ddot{q}_t - \alpha \ddot{q}_{t+\Delta t} \right] \Delta t^2$$
(20)

The parameters  $\alpha$  and  $\delta$  are for stability and accuracy of integration and are equal to  $\alpha = \frac{1}{6}$  and  $\delta = \frac{1}{2}$ . To find  $\mathbf{q}_{t+\Delta t}$ , Newmark's method involves solving the system:

$$\hat{\mathbf{K}}\mathbf{q}_{t+\Delta t} = \hat{\mathbf{R}}_{t+\Delta t} \tag{21}$$

where  $\hat{\mathbf{K}}$  is the effective stiffness matrix:

$$\hat{\mathbf{K}} = \mathbf{K} + \frac{1}{\alpha(\Delta t)^2} \mathbf{M} + \frac{\delta}{\alpha \Delta t} \mathbf{C}$$
 (22)

and  $\hat{\mathbf{R}}_{t+\Delta t}$  are the effective loads:

$$\hat{\mathbf{R}}_{t+\Delta t} = \mathbf{R}_{t+\Delta t} + \mathbf{M} \left( \frac{1}{\alpha (\Delta t)^2} \mathbf{q}_t + \frac{1}{\alpha \Delta t} \dot{\mathbf{q}}_t + \left( \frac{1}{2\alpha} - 1 \right) \ddot{\mathbf{q}}_t \right)$$

$$+ \mathbf{C} \left( \frac{\delta}{\alpha \Delta t} \mathbf{q}_t + \left( \frac{\delta}{\alpha} - 1 \right) \dot{\mathbf{q}}_t + \frac{\Delta t}{2} \left( \frac{\delta}{\alpha} - 2 \right) \ddot{\mathbf{q}}_t \right)$$
(23)

After finding the solution  $\mathbf{q}_{t+\Delta t}$ , one can also calculate the derivatives in time  $\dot{\mathbf{q}}_{t+\Delta t}$  and  $\ddot{\mathbf{q}}_{t+\Delta t}$  via Eq. 20. The same procedure is repeated for each time-step. More details can be found in [25].

#### 3. Numerical results

In this section, some numerical results are presented for a simple isotropic beam [20]. For representative purposes, first a coupled thermoelastic static analysis and then, a transient quasi-static analysis are proposed.

## 3.1 Static coupled thermoelastic analysis

The case examined [20] is a cantilever beam with a square cross section, whose area is  $A=20~\rm cm^2$  and length is  $L=50~\rm cm$ . The material of the beam is aluminum and it has the following characteristics: Young's modulus  $E=73.1~\rm GPa$ , Poisson's coefficient v=0.33, coefficient of thermal expansion  $\alpha=23.1\times10^{-6}~\rm K^{-1}$  and thermal conductivity  $\kappa=237~\rm W/(m~\rm K)$ . A heat flux of  $q=100~\rm W$  is applied at the clamped edge, while the free edge is left at room temperature.

Displacements along *y* and temperature changes are calculated at different sections along the beam. The number of 4-node beam elements for two different lagrange expansions (one element L9 and one L16 on the cross-section) is varied to evaluate the convergence of the results (Tables 1 and 2). Table 3 then shows the results obtained using second-, third- and fourth-order Taylor models in the case where the beam is discretized with 30 B4 elements.

The results obtained are in obvious agreement with those obtained in [20]. It can be seen from the results that it takes only a few elements to already achieve good accuracy of results.

The Fig. 1 shows how displacements and temperature along the beam vary for the 30 B4/1L9 model.

|                   | Location along y-axis [m]   |              |                |                |                |                |              |         |
|-------------------|-----------------------------|--------------|----------------|----------------|----------------|----------------|--------------|---------|
| Number of FEs     |                             | 0.0          | 0.1            | 0.2            | 0.3            | 0.4            | 0.5          | DOF     |
| 5 B4              | u <sub>y</sub> [mm]         | 0.0          | 0.242          | 0.411          | 0.532          | 0.606          | 0.630        | <br>576 |
| J D4              | $T \ [^{\circ}C]$           | 105.5        | 84.4           | 63.3           | 42.2           | 21.1           | 0.0          | 370     |
| 10 B4             | $u_y [mm]$ $T [^{\circ}C]$  | 0.0<br>105.5 | 0.235<br>84.4  | 0.405<br>63.3  | 0.527<br>42.2  | 0.600<br>21.1  | 0.625<br>0.0 | 1116    |
| 20 B4             | $u_y [mm] $ $T [^{\circ}C]$ | 0.0<br>105.5 | 0.234<br>84.4  | 0.404<br>63.3  | 0.526<br>42.2  | 0.599<br>21.1  | 0.624<br>0.0 | 2196    |
| 30 B4             | $u_y [mm] $ $T [^{\circ}C]$ | 0.0<br>105.5 | 0.234<br>84.4  | 0.404<br>63.3  | 0.526<br>42.2  | 0.599<br>21.1  | 0.624<br>0.0 | 3276    |
| Ref. [20] (20 B4) | $u_y [mm] $ $T [^{\circ}C]$ | 0.0<br>105.5 | 0.232<br>84.38 | 0.403<br>63.28 | 0.525<br>42.19 | 0.599<br>21.09 | 0.622<br>0.0 |         |

Table 1 – Displacement in y-direction and temperature change along the beam axis as the number of finite elements changes for a 1L9 model.

|                   | Location along y-axis [m]   |              |                |                |                |                |              |      |
|-------------------|-----------------------------|--------------|----------------|----------------|----------------|----------------|--------------|------|
| Number of FEs     |                             | 0.0          | 0.1            | 0.2            | 0.3            | 0.4            | 0.5          | DOF  |
| 5 B4              | $u_y$ $[mm]$                | 0.0          | 0.242          | 0.411          | 0.532          | 0.605          | 0.630        | 1024 |
| 3 04              | $T [^{\circ}C]$             | 105.5        | 84.4           | 63.3           | 42.2           | 21.1           | 0.0          | 1024 |
| 10 B4             | $u_y [mm]$ $T [^{\circ}C]$  | 0.0<br>105.5 | 0.234<br>84.4  | 0.405<br>63.3  | 0.527<br>42.2  | 0.600<br>21.1  | 0.624<br>0.0 | 1984 |
| 20 B4             | $u_y [mm] $ $T [^{\circ}C]$ | 0.0<br>105.5 | 0.233<br>84.4  | 0.403<br>63.3  | 0.525<br>42.2  | 0.598<br>21.1  | 0.622<br>0.0 | 3904 |
| 30 B4             | $u_y [mm] $ $T [^{\circ}C]$ | 0.0<br>105.5 | 0.232<br>84.4  | 0.403<br>63.3  | 0.525<br>42.2  | 0.598<br>21.1  | 0.622<br>0.0 | 5824 |
| Ref. [20] (20 B4) | $u_y [mm] $ $T [^{\circ}C]$ | 0.0<br>105.5 | 0.231<br>84.38 | 0.402<br>63.28 | 0.524<br>42.19 | 0.597<br>21.09 | 0.621<br>0.0 | _    |

Table 2 – Displacement in y-direction and temperature change along the beam axis as the number of finite elements changes for a 1L16 model.

|       | Location along y-axis [m]  |              |               |               |               |               |              |      |  |
|-------|----------------------------|--------------|---------------|---------------|---------------|---------------|--------------|------|--|
| Model |                            | 0.0          | 0.1           | 0.2           | 0.3           | 0.4           | 0.5          | DOF  |  |
| TE2   | $u_y$ [mm]                 | 0.0          | 0.234         | 0.404         | 0.526         | 0.599         | 0.624        | 2184 |  |
| ILZ   | $T [^{\circ}C]$            | 105.5        | 84.4          | 63.3          | 42.2          | 21.1          | 0.0          | 2104 |  |
| TE3   | $u_y [mm]$ $T [^{\circ}C]$ | 0.0<br>105.5 | 0.232<br>84.4 | 0.403<br>63.3 | 0.525<br>42.2 | 0.598<br>21.1 | 0.622<br>0.0 | 3640 |  |
| TE4   | $u_y [mm] $ $T [°C]$       | 0.0<br>105.5 | 0.232<br>84.4 | 0.403<br>63.3 | 0.524<br>42.2 | 0.598<br>21.1 | 0.622<br>0.0 | 5460 |  |
| 1L9   | $u_v [mm]$                 | 0.0          | 0.234         | 0.404         | 0.526         | 0.599         | 0.624        |      |  |
|       | $T [^{\circ}C]$            | 105.5        | 84.4          | 63.3          | 42.2          | 21.1          | 0.0          | 3276 |  |
| 1L16  | $u_v [mm]$                 | 0.0          | 0.232         | 0.403         | 0.525         | 0.598         | 0.622        | F004 |  |
|       | $T [^{\circ}C]$            | 105.5        | 84.4          | 63.3          | 42.2          | 21.1          | 0.0          | 5824 |  |

Table 3 – Displacement in the *y*-direction and temperature change along the beam axis as the Taylor model and Lagrange model changes for the 30 B4 case.

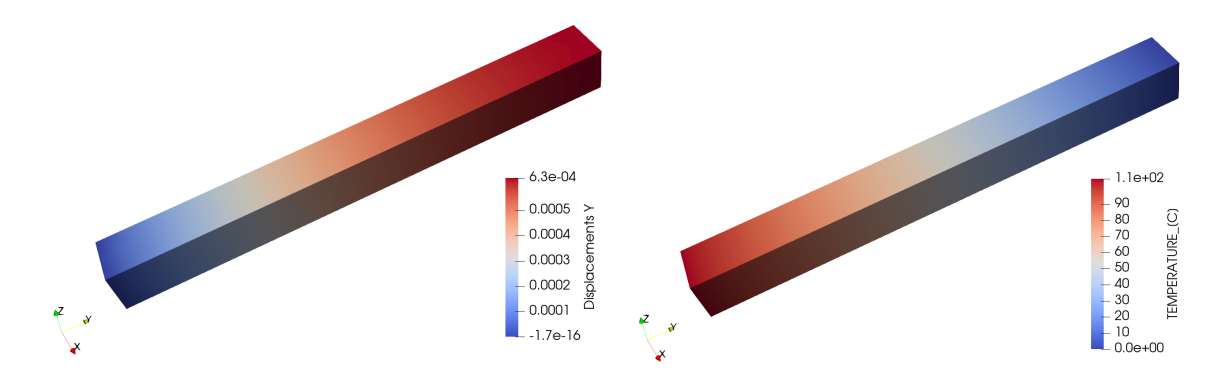


Figure 1 – Displacement and temperature variation along the beam for the 30 B4/1L9 model.

## 3.2 Transient quasi-static analysis

The same configuration is considered as in the static case [20]. Inertial effects are not considered in this analysis. In addition, the coefficients of the governing equations  $t_0$ ,  $t_1$ ,  $t_2$  and  $\tilde{c}$  are null. The heat capacity is equal to  $c = 903 \, \mathrm{J/(kg \, K)}$ .

We consider a model with 5 B4 finite elements and a Lagrange expansion on cross-section 1L9. Fig. 2 show the displacements and temperature changes over time for different positions along the y-axis. After a short transient, the stationary solution obtained in the previous paragraph (Table 1) is reached. The Fig. 3 shows the temperature trend along the beam for different times.

### 4. Conclusion

This paper presented the study of coupled thermoelasticity of isotropic and homogeneous beams. The static and quasi-static problems are analyzed starting from the generalized governing equations. The results show that the use of refined 1D models based on the Carrera Unified Formulation allows the accurate evaluation of displacements and temperature changes for a structure subjected to heat flow and with lower computational costs than 3D models. In addition, it was possible to compare the results for different polynomial expansions of Lagrange and Taylor types. The convergence rate is excellent for Lagrange models. It takes only five beam elements to find the correct temperature value and ten elements to predict displacements. In addition, the results show that the use of Taylor models also allow to obtain a good accuracy even with low orders ( $N \ge 3$ ) and with computational costs usually lower than Lagrange models.

In future work, it will be possible to include the study of thermal shock phenomena using coupled thermoelasticity.

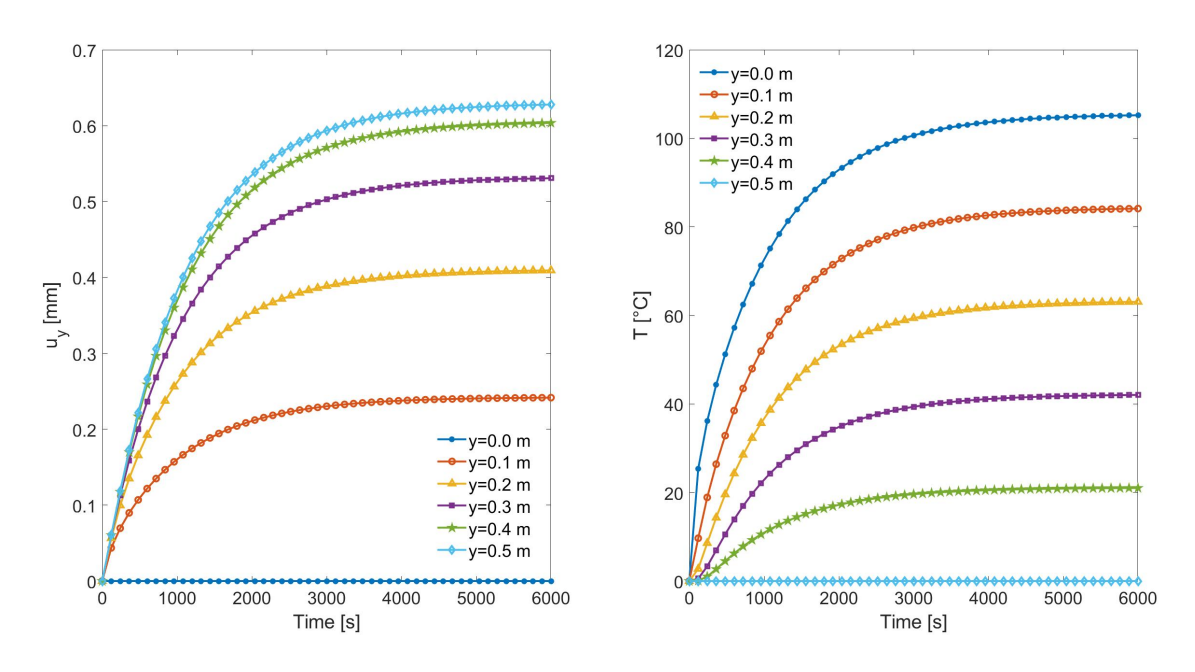


Figure 2 – Displacements and temperature changes over time for different positions along the *y*-axis.

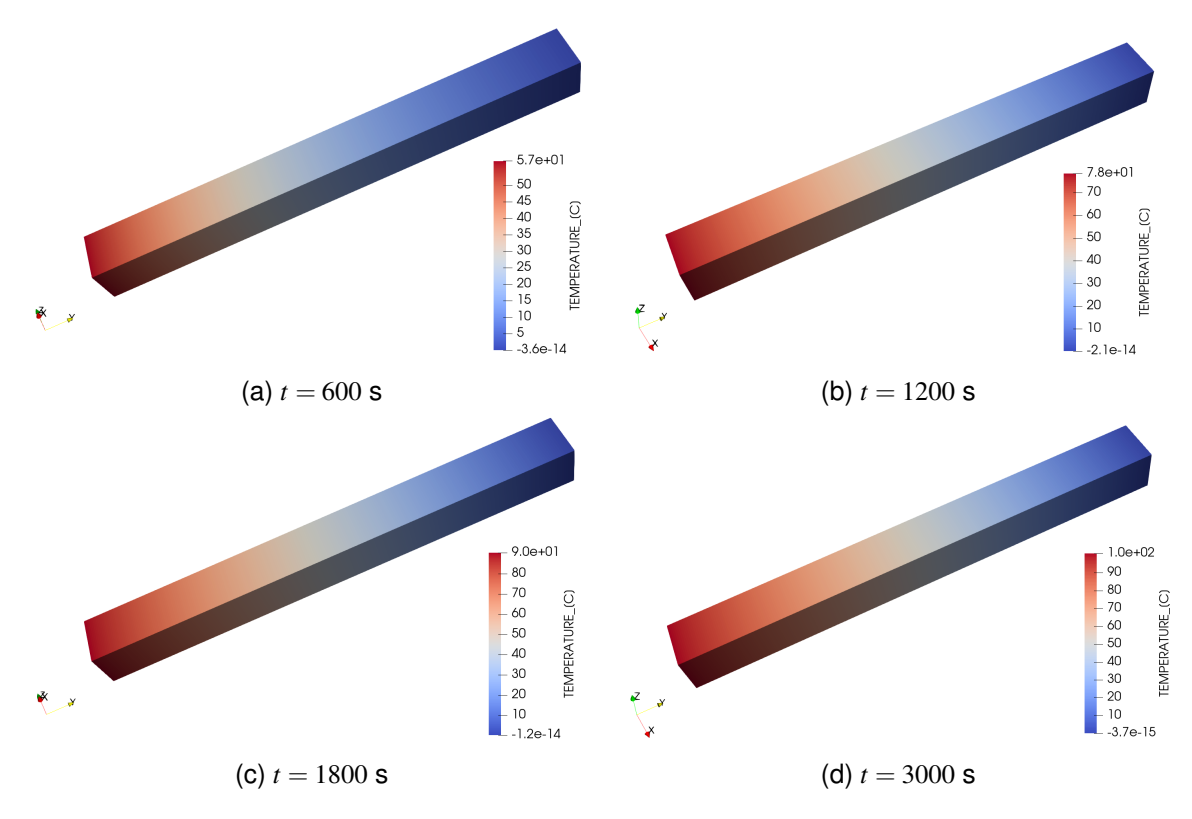


Figure 3 – Temperature variation along the beam at different times.

# 5. Contact Author Email Address

Mailto: matteo.filippi@polito.it (M. Filippi).

# 6. Copyright Statement

The authors confirm that they, and/or their company or organization, hold copyright on all of the original material included in this paper. The authors also confirm that they have obtained permission, from the copyright holder of any third party material included in this paper, to publish it as part of their paper. The authors confirm that they give permission, or have obtained permission from the copyright holder of this paper, for the publication and distribution of this paper as part of the ICAS proceedings or as individual off-prints from the proceedings.

#### References

- [1] Duhamel, J. M. Second Memoire Sur Les Phenomenes Thermo-Mecaniques. *Journal de l'Ecole Polytechnique*, Vol. 15, pp 1–57, 1937.
- [2] Biot, M. A. Thermoelasticity and irreversible thermodynamics. *Journal of applied physics*, Vol 27, pp 240-253, 1956.
- [3] Lord, H. W. and Shulman, Y. A generalized dynamical theory of thermoelasticity, *Journal of the Mechanics and Physics of Solids*, Vol. 15, pp 299–309, 1967.
- [4] Green, A. E. and Lindsay, K. A. Thermoelasticity. *Journal of elasticity*, Vol. 2, pp 1–7, 1972.
- [5] Hetnarski, R. B., Eslami, R. M. and Gladwell, G. M. L. Thermal stresses: advanced theory and applications. *Berlin: Springer*, Vol. 41, 2009.
- [6] Abbas, I. A. and Marin, M. Analytical solutions of a two-dimensional generalized thermoelastic diffusions problem due to laser pulse. *Iranian Journal of Science and Technology, Transactions of Mechanical En*gineering, Vol. 42, pp 57-71, 2018.
- [7] Kakhki, E. K., Hosseini, S. M. and Tahani, M. An analytical solution for thermoelastic damping in a microbeam based on generalized theory of thermoelasticity and modified couple stress theory. *Applied Mathematical Modelling*, Vol. 40(4), pp 3164-3174, 2016.
- [8] Entezari, A. and Kouchakzadeh, M. A. Analytical solution of generalized coupled thermoelasticity problem in a rotating disk subjected to thermal and mechanical shock loads. *Journal of Thermal Stresses*, Vol. 39.12, pp 1588-1609, 2016.
- [9] Carrera, E., Cinefra, M., Petrolo, M. and Zappino, E. Finite element analysis of structures through unified formulation. *John Wiley & Sons*, 2014.
- [10] Nagaraj, M.H., Kaleel, I., Carrera, E., Petrolo, M.: Elastoplastic Micromechanical Analysis of Fiber-Reinforced Composites with Defects. Aerotec. Missili Spaz. 101, 53-59 (2022). https://doi.org/10.1007/s42496-021-00103-4.
- [11] Kaleel, I., Petrolo, M., Carrera, E. Elastoplastic and progressive failure analysis of fiber-reinforced composites via an efficient nonlinear microscale model. Aerotec. Missili Spaz. 97, 103-110 (2018). https://doi.org/10.1007/BF03405805.
- [12] Scano, D., Carrera, E., Petrolo, M. Use of the 3D Equilibrium Equations in the Free-Edge Analyses for Laminated Structures with the Variable Kinematics Approach. Aerotec. Missili Spaz. 103(2), 179-195 (2024). https://doi.org/10.1007/s42496-023-00177-2.
- [13] Pagani, A., Racionero Sanchèz Majano, A., Zamani, D., Petrolo, M., Carrera, E. Fundamental Frequency Layer-Wise Optimization of Tow-Steered Composites Considering Gaps and Overlaps. Aerotec. Missili Spaz. In Press. https://doi.org/10.1007/s42496-024-00212-w.
- [14] Petrolo, M., Iannotti, P. Best Theory Diagrams for Laminated Composite Shells Based on Failure Indexes. Aerotec. Missili Spaz. 102, pp. 199-218 (2023). https://doi.org/10.1007/s42496-023-00158-5.
- [15] Carrera, E. Theories and finite elements for multilayered plates and shells: a unified compact formulation with numerical assessment and benchmarking. *Archives of Computational Methodsin Engineering*, Vol. 10(3), pp 215-296, 2003.
- [16] Carrera, E. and Giunta, G. Refined beam theories based on a unified formulation. *International Journal of Applied Mechanics*, Vol. 2(1), pp 117-143, 2010.
- [17] Carrera, E. and Nali, P. Multilayered plate elements for the analysis of multifield problems. *Finite Elements in Analysis and Design*, Vol. 46(9), pp 732-742, 2010.
- [18] Carrera, E., Cinefra, M. and Fazzolari, F. A. Some results on thermal stress of layered plates and shells by using unified formulation. *Journal of Thermal Stresses*, Vol. 36(6), pp 589-625, 2013.
- [19] Carrera, E. and Petrolo, M. Computational models for the multifield analysis of laminated shells and related best theory diagrams. *Shell Structures: Theory and Applications Volume 4*, CRC Press, pp 3-9, 2017.
- [20] Filippi, M., Entezari, A. and Carrera, E. Unified finite element approach for generalized coupled thermoe-

# **COUPLED THERMOELASTIC ANALYSIS OF BEAM STRUCTURES**

- lastic analysis of 3D beam-type structures, part 2: Numerical evaluations. *Journal of Thermal Stresses*, Vol. 40.11, pp 1402-1416, 2017.
- [21] Entezari, A., Filippi, M., Carrera, E., Kouchakzadeh, M. A. 3D dynamic coupled thermoelastic solution for constant thickness disks using refined 1D finite element models. *Applied Mathematical Modelling*, Vol. 60, pp 273-285, 2018.
- [22] Entezari, A., Filippi, M., Carrera, E., Kouchakzadeh, M. A. 3D-wave propagation in generalized thermoelastic functionally graded disks. *Composite Structures*, Vol. 206, pp 941-951, 2018.
- [23] Li, Z., Ma, Q. and Cui, J. Finite element algorithm for dynamic thermoelasticity coupling problems and application to transient response of structure with strong aerothermodynamic environment. *Communications in Computational Physics*, Vol. 20(3), pp 773-810, 2016.
- [24] Entezari, A., Filippi, M., and Carrera, E. Unified finite element approach for generalized coupled thermoelastic analysis of 3D beam-type structures, part 1: Equations and formulation. *Journal of Thermal Stresses*, Vol. 40.11, pp 1386-1401, 2017.
- [25] Bathe, K. J. Finite element procedures. Klaus-Jurgen Bathe, 2006.